

Ultrashort Peptides for the Self-Assembly of an Antiviral Coating

Tan Hu, Michaela Kaganovich, Zohar Shpilt, Apurba Pramanik, Omer Agazani, Siyi Pan, Edit Tshuva, and Meital Reches*

Antiviral compounds are important for generating sterile surfaces. Here, two extremely short peptides, DOPA-Phe-NH $_2$ and DOPA-Phe(4F)-NH $_2$ that can self-assemble into spherical nanoparticles with antiviral activity are presented. The peptide assemblies possess excellent antiviral activity against bacteriophage T4 with antiviral minimal inhibitory concentrations of 125 and 62.5 μ g mL $^{-1}$, for DOPA-Phe-NH $_2$ and DOPA-Phe(4F)-NH $_2$, respectively. When the peptide assemblies are applied on a glass substrate by dropcasting, they deactivate more than 99.9% of bacteriophage T4 and Canine coronavirus. Importantly, the peptide assemblies have low toxicity toward mammalian cells. Overall, the findings can provide a novel strategy for the design and development of antiviral coatings for a decreased risk of viral infections.

1. Introduction

The continuous emergence of deadly viral outbreaks such as the seasonal flu virus A, Ebola virus, and the novel coronavirus 2019 (COVID-19) have greatly increased the need for novel effective antiviral technologies.^[1-4] To date, numerous antiviral compounds have been successfully developed and approved

T. Hu, M. Kaganovich, Z. Shpilt, A. Pramanik, O. Agazani, E. Tshuva, M. Reches Institute of Chemistry and The Center for Nanoscience and Nanotechnology The Hebrew University of Jerusalem Jerusalem 91904, Israel E-mail: meital.reches@mail.huji.ac.il T. Hu, S. Pan College of Food Science and Technology Huazhong Agricultural University Wuhan, Hubei 430070, P. R. China T. Hu. S. Pan Key Laboratory of Environment Correlative Dietology Huazhong Agricultural University Ministry of Education Wuhan, Hubei 430070, P. R. China

The ORCID identification number(s) for the author(s) of this article can be found under https://doi.org/10.1002/admi.202202161.

© 2023 The Authors. Advanced Materials Interfaces published by Wiley-VCH GmbH. This is an open access article under the terms of the Creative Commons Attribution License, which permits use, distribution and reproduction in any medium, provided the original work is properly cited.

DOI: 10.1002/admi.202202161

for clinical use. These compounds inhibit essential enzymatic processes that are involved in viral replication and entry/ fusion (e.g., Oseltamivir and Zanamivir) while others are immunomodulatory drugs (e.g., interferon).^[5,6] However, the currently available antiviral compounds exhibit low or no efficacy against viral infections according to the increasing number of reports on viral resistance, coinfections, and the emergence of viral epidemics such as COVID-19.[5-8] Therefore, there is a high demand for developing novel antiviral agents and approaches that can serve as a supplement or an alternative to existing drugs.

Many research efforts have been made toward the development of vaccines and drugs against novel viruses due to COVID-19 pandemic outbreak. [9-13] However, it is still challenging to reduce the risk, at the early stage of the viral outbreak, with these approaches. Viral pathogens especially respiratory infection viruses can be transmitted through respiratory droplets, aerosols, or contacts.[14,15] These viruses can adhere and survive on surfaces, both in healthcare settings and on common surfaces, for days and months. [16,17] Touching contaminated surfaces poses a great risk for viral transmission via the surface route. Therefore, it is an urgent need to develop effective antiviral coatings that prevent the survival of viruses on surfaces. It has been reported that coatings modified by antiviral natural extractions, [18] antiviral polymers, [19] metal ions, oxides, [20] and nanomaterials [21] show excellent antiviral activity to reduce viral infection. However, some of them pose potential hazards to the environment and human health.

Peptides can be exploited as new and improved antiviral agents due to their biocompatibility and low cytotoxicity. $^{[22-27]}$ Daher et al. demonstrated an antimicrobial peptide (α -defensin) that inhibits herpes simplex virus types 1 and 2, cytomegalovirus, and vesicular stomatitis virus. $^{[28]}$ Xia and his colleagues designed a 36-residue peptide termed EK1 as an antiviral peptide against SARS-CoV, MERS-CoV, and three SARS-related CoVs. $^{[29]}$

Still, to be applied as a coating these peptides need to adhere to the surface, and have low manufacturing cost for adequate large-scale production.^[30] The shorter the peptide is, the easier it is to synthesize and the production is much less expensive. Therefore, extremely short peptides that exhibit effective antiviral activity can be utilized for generating antiviral coatings.



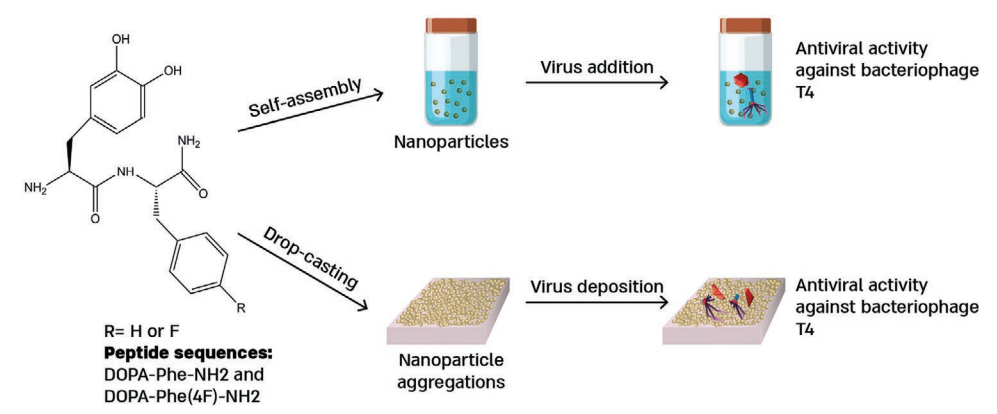


Figure 1. The scheme illustrates the formation of peptide-based assemblies and peptide coatings with antiviral activity.

We have recently demonstrated that the tripeptides DOPA-Phe-Phe-OMe and DOPA-Phe(4F)-Phe(4F)-OMe self-assemble into spherical particles that when applied on surfaces provide antiviral activity against both a DNA-based virus (bacteriophage T4) and an RNA-based virus (canine coronavirus, (CCV)).[31] The antiviral activity results from the specific spherical supramolecular structure of the peptides. Reducing the length of the tripeptides to a minimal two amino acids is of high interest and relevance as it significantly reduces their cost and makes them more appealing for use in many fields including agriculture, food packaging, and cosmetics. Here, we present extremely short peptides comprising only two amino acids with antiviral capabilities. Importantly, we show that even a non-fluorinated dipeptide can form an antiviral coating. Fluorinated polymers are being widely used today due to their low surface tension, hydrophobicity, and antifouling properties.^[31] However, it has been reported that consuming a dose larger than 10 mg per day of fluorinated compounds can be toxic and potentially results in skeletal fluorosis and gastrointestinal side effects. Thus it is highly important to avoid the leaching of fluorinated compounds.^[32] Both dipeptides self-assemble into supramolecular structures that show excellent antiviral activity in solution and on a surface as a coating (Figure 1). These findings can provide a novel strategy for the design and development of ultrashort peptides as antiviral coatings for decreasing viral infections.

2. Results and Discussion

Two dipeptides, DOPA-Phe-NH₂ and DOPA-Phe(4F)-NH₂, were examined for their antiviral activity in solution and as a coating. The two peptides comprise one 3,4-dihydroxy-L-phenylalanine (DOPA) and one phenylalanine or fluorinated phenylalanine. L-DOPA is the main constituent of mussel adhesive proteins that can adhere to almost any substrate and can function under harsh conditions. Phenylalanine and fluorinated phenylalanine are aromatic amino acids that can mediate peptide self-assembly through π – π stacking (Figure 1).

To investigate the antiviral activity of DOPA-Phe-NH $_2$ and DOPA-Phe(4F)-NH $_2$ in solution, we performed an assay to identify the antiviral minimal inhibitory concentration (antiviral MIC) of each peptide. We first dissolved the peptides in ethanol to a concentration of 100 mg mL $^{-1}$ and then diluted it with

triple distilled water to several concentrations. Both DOPA-Phe-NH2 and DOPA-Phe(4F)-NH2 exhibited antiviral activity against bacteriophage T4 (Table 1). Bacteriophage T4 is one of the most commonly used models for assessing antiviral activity against DNA-based viruses.[34,35] It is a relatively large, nonenveloped 170 kbp double-stranded DNA virus.^[34] The antiviral MIC was 125 and 62.5 µg mL⁻¹ for DOPA-Phe-NH₂ and DOPA-Phe(4F)-NH2, respectively, indicating that DOPA-Phe(4F)-NH2 had better antiviral activity than DOPA-Phe-NH₂. This suggests that fluorinated residues can enhance the antiviral activity of the peptide. It follows our previous report on self-assembled tripeptides that have a similar antiviral activity with antiviral MIC of tens of µg mL⁻¹.[31] The antiviral MIC against bacteriophage T4 for the tripeptides DOPA-Phe(4F)-Phe(4F)-OMe and DOPA-Phe-Phe-OMe was 31 and 62 µg mL⁻¹, respectively. Although the tripeptides and dipeptides show comparative antiviral MIC against bacteriophage T4, the dipeptides are easier to synthesize and have a lower cost when compared with the tripeptides.

The importance of phenylalanine and fluorinated phenylalanine in antiviral peptides has been reported before. [36] Incorporating one or several fluorine atoms into an organic molecule can improve the pharmacokinetic and pharmacodynamic properties such as absorption, tissue distribution, secretion, the route and rate of biotransformation, toxicology, bioavailability, metabolic stability, and lipophilicity. [36] Specifically, it was demonstrated that the peptide carbobenzoxy-Dphenylalanine-L-phenylalanine-glycine acts as an inhibitor

Table 1. Antiviral MIC for L-amino acids and dipeptides.

Peptide sequences	Antiviral MIC [µg mL ⁻¹]
L-DOPA	=
L-Phe	-
L-Phe(4F)	-
DOPA-Phe-NH ₂	125.00
DOPA-Phe(4F)-NH ₂	62.50
Diphenylalanine	-
Phe(4F)-Phe(4F)-Ome	-
CuNPs	2500

[&]quot;-" represents no antiviral activity.



of membrane fusion.[37] In addition, it was shown that the fluoro-group at the phenyl ring in a triazole-dipeptide hybrid is essential for the antiviral activity of the peptide. [37] To explore the antiviral mechanism for the dipeptide assemblies, we also evaluated the antiviral activity against bacteriophage T4 for L-DOPA, L-phenylalanine(L-Phe), fluorinated phenylalanine (L-Phe(4F)), diphenylalanine (Phe-Phe), and fluorinated diphenylalanine (Phe(4F)-Phe(4F)-OMe). As shown in Table 1, a single amino acid and the dipeptides Phe-Phe and Phe(4F)-Phe(4F)-OMe did not decrease the viral titer. We included copper nanoparticles (CuNPs) as a positive control in the antiviral MIC experiment. We chose these particles over antiviral drugs as they are not specific toward a certain viral strain and due to their similar spherical morphology and size.^[5] The antiviral MIC for CuNPs is 2500 µg mL⁻¹ much higher than the peptides MIC. This means that the peptides are much more effective as antiviral

To investigate in what form the peptides exist in the solution at the MIC concentration, a transmission electron microscope (TEM) was used. The TEM analysis for the dipeptide DOPA-Phe-NH₂ revealed that the peptide self-assembles into spherical nanoparticles with a size ranging from several nanometers up to 20 nm (Figure 2a). Using scanning electron microscopy (SEM) and atomic force microscopy (AFM) (Figure 2b,c) we were able to detect spherical structures with a diameter of 10-50 nm. Interestingly, there was no appreciable effect on the particle size when comparing DOPA-Phe-NH₂ and DOPA-Phe(4F)-NH₂, indicating that fluorine modification on the benzene ring of the Phe residue did not influence the peptide self-assembly (Figure 2d-f). The slight difference in size between TEM and

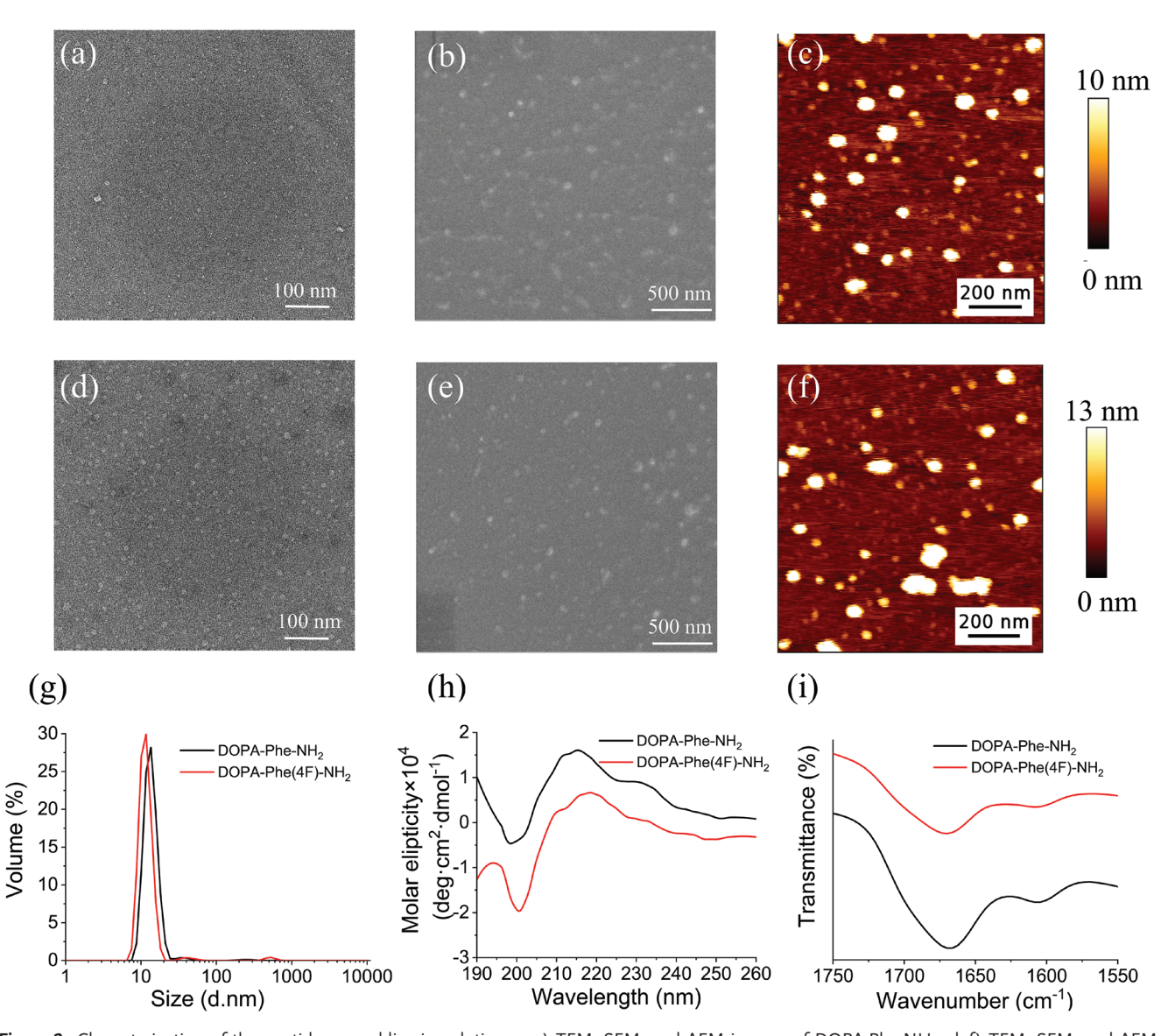


Figure 2. Characterization of the peptide assemblies in solution. a-c) TEM, SEM, and AFM images of DOPA-Phe-NH₂, d-f) TEM, SEM, and AFM images of DOPA-Phe(4F)-NH2, g) DLS size distribution for DOPA-Phe-NH2 and DOPA-Phe(4F)-NH2, h) CD spectra, and i) FTIR spectrum (Amide I) for DOPA-Phe-NH₂ and DOPA-Phe(4F)-NH₂.



ADVANCED MATERIALS INTERFACES Www.advmatinterfaces.de

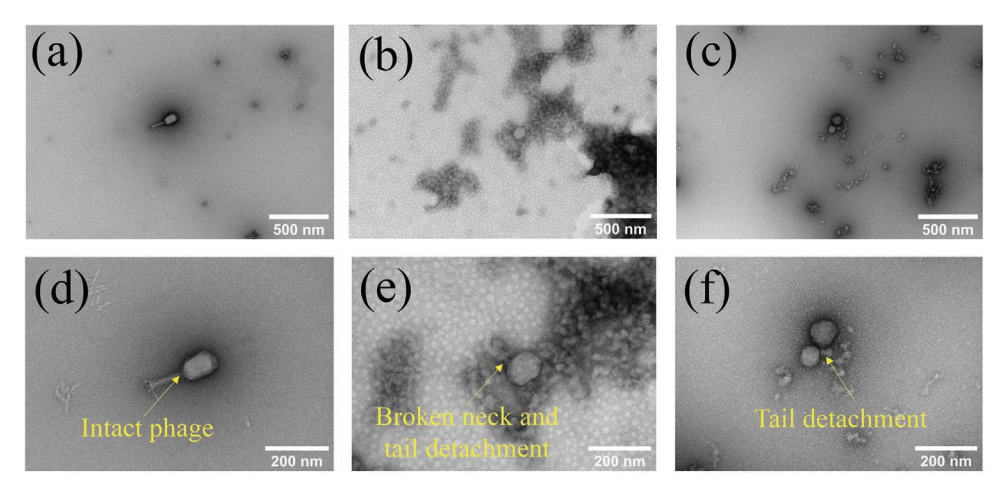


Figure 3. TEM images at different magnifications of a,d) untreated T4 bacteriophages, b,e) treated with DOPA-Phe-NH₂, and c,f) treated with DOPA-Phe(4F)-NH₂.

SEM analysis may result from the sample preparation procedure where for TEM the sample is dried on a grid and negatively stained using uranyl acetate. Dynamic light scattering (DLS) analysis that is performed in solution revealed that the size of the self-assembled structures ranges from 10 to 50 nm. (Figure 2g). Circular Dichroism (CD) and Fourier-transform infrared (FT-IR) spectroscopy were used to determine the secondary structure of the peptides (Figure 2h,i). The CD spectra of both peptides exhibited a negative peak at ≈200 nm and a positive peak at \approx 215 nm. This result suggests a β -turn configuration for the peptide assemblies.^[38] Furthermore, the FT-IR spectra for DOPA-Phe-NH2 and DOPA-Phe(4F)-NH2 showed a distinct peak at around 1668 and 1670 cm⁻¹, respectively, implying a β -turn configuration.^[39] Overall, these results suggest that introducing fluorinated atoms into the peptide sequence does not change the structure of the assemblies. The ordered structures could be formed by the π - π stacking between the aromatic residues, hydrogen bonds, and electrostatic interactions between the N- and C-termini.

To better understand the mechanism of the antiviral activity, we incubated a solution of bacteriophage T4 with the peptide assemblies at the antiviral MIC for 24 h and performed a TEM analysis (Figure 3b,c,e and f). As a control, a solution of bacteriophage T4 without any peptide was analyzed (Figure 3a,d). In this control sample, the bacteriophages exhibited a typical structure of the viral head, tail, and long tail fibers. In contrast, when the bacteriophages were exposed and incubated with the peptide assemblies, the tail was detached from the head (Figure 3b,c,e and f and Figure S3b-j, Supporting Information). This detachment was detected with both types of peptide assemblies (marked with an arrow). The head of bacteriophage T4 is attached to the tail via the neck proteins gp13 and gp14; subsequently, six 500 Å long, trimeric "whisker" fibers (gpWac) are attached to the neck.[40] Based on this information, we suggest that by interacting with the neck proteins, the peptide assemblies can disturb the protein structure. Moreover, significant damage to the morphology of the head could also be observed (Figure 3b,c,e and f); the head did not exhibit an elongated icosahedron compared with the bacteriophages that were not exposed to the assemblies. We suggest that the damage to the morphology of the head could be due to the interaction and disruption between the bacteriophage capsid and the peptide assemblies.^[41] Importantly, the long tail fibers were also separated from the T4 tail. It has been reported that the long tail fiber consists of four proteins (gp34, gp35, gp36, and gp37) that recognize the receptor-binding site on the host cell.^[41] The destruction of the long tail fibers could lead to unrecognition for *Escherichia coil 11303* and could cause deactivation.^[42] As a positive control, we also examined the morphology of bacteriophages exposed to copper NPs (CuNPs) at an antiviral MIC. TEM analysis indicates that the CuNPs can also destroy the viral structures (Figure S1, Supporting Information).

To further utilize the self-assembled particles to generate an antiviral coating, we used a protocol we reported before.[31] A peptide solution of DOPA-Phe-NH₂ or DOPA-Phe(4F)-NH₂, at a concentration of 10 mg mL⁻¹, was drop-casted three times on a clean glass substrate. This process resulted in transparent surfaces (Figure 4a). SEM analysis reveals aggregates of spherical nanoparticles formed by DOPA-Phe-NH2 on the surface (Figure 4c). This aggregation is probably due to the high concentration of assemblies and the drying process. AFM topography images show that the aggregates are not uniform (Figure 4d). Similar aggregated structures were obtained by DOPA-Phe(4F)-NH2 (Figure 4e,f). The attenuated total reflectance fourier transform infrared (ATR-FTIR) spectra of the assemblies formed on the surface by the peptides are shown in Figure 4b. The IR region 1800–1500 cm⁻¹ is associated with the stretching band of amide I and indicates the secondary structure of the peptides (Figure S2, Supporting Information). The ATR-FTIR spectrum of a glass substrate coated with DOPA-Phe-NH₂ had one main peak at 1666 cm⁻¹, indicating a β -type structure. [43,44] For the DOPA-Phe(4F)-NH2 coating, a similar peak appeared at 1669 cm⁻¹; this suggests that both peptides form similar assemblies on the surface.

We investigated the antiviral activity of the peptide-based coatings against both bacteriophage T4 and CCV. A solution of bacteriophages at a concentration of 1.0×10^6 plaque-forming units (PFU) mL⁻¹ was applied on the peptide-based coating and incubated for 24 h. Then, the virus titer was determined by counting the number of plaques. As shown in Figure 4g, no

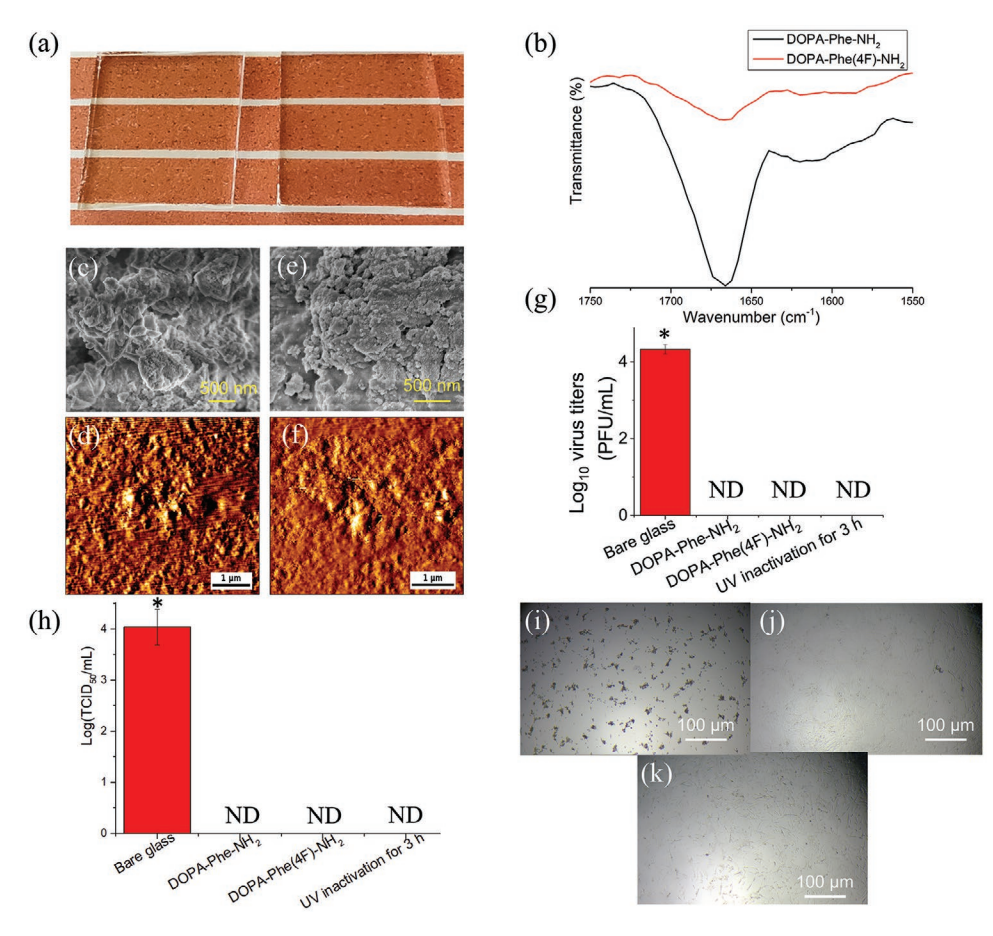


Figure 4. Characterization of the peptide assemblies on the surface and their antiviral activity against bacteriophage T4 and CCV. a) Images of surfaces (1 x 1 cm) coated by DOPA-Phe-NH2 (on the left) and DOPA-Phe(4F)-NH2 (on the right), b) ATR-FTIR spectrum for coatings formed by DOPA-Phe-NH2 or DOPA-Phe(4F)-NH2, c,d) SEM and AFM images for coatings of DOPA-Phe-NH2, e,f) SEM and AFM images of DOPA-Phe(4F)-NH2, g) Antiviral activity for the peptide-based coatings against bacteriophage T4, h) Antiviral activity for peptide-based coatings against CCV, i-k) Representative infected cells on bare glass, DOPA-Phe-NH2 and DOPA-Phe(4F)-NH2 coatings. "*" represents that ANOVA and Duncan's test were used to indicate the statistically significant differences among values (p < 0.05). "ND" represents "no virus was detected."

viruses were detected on the coatings formed by either DOPA-Phe-NH₂ or DOPA-Phe(4F)-NH₂. On a bare glass, the viral titer was $29\,000 \pm 2000$ PFU mL⁻¹ and from that, we can deduce that the peptide-based coatings can reduce the viral titer by nearly 4 logs. This suggests that both peptide coatings can deactivate more than 99.9% of the viruses (p < 0.05). A surface with T4 bacteriophage was treated by UV inactivation for 3 h and served as a positive control. A bare glass washed with ethanol was used as a negative control to confirm that the antiviral activity is from the peptide itself. The virus titers treated by UV light were below the limit of detection.

Importantly, we carried out an antiviral activity assay against CCV. To examine the antiviral activity of the peptide with coronavirus, we used a corona surrogate CCV. This is an enveloped, positive-stranded RNA virus with specific sequence homology to SARS-CoV-2. As shown in Figure 4h, no virus could be detected for both peptide-based coatings. When we compared the peptide-based coatings with a bare glass (log (TCID₅₀) per mL) = 4.04 ± 0.39), the peptide coatings could reduce the amount of CCV by more than 99.9% (p < 0.05). This indicated that the coating inactivated both bacteriophage T4 and CCV.

Adv. Mater. Interfaces 2023, 10, 2202161

Our previous work showed that a coating formed by tripeptides can also inactivate these viruses.[31] Therefore, these DOPA-based di-/tripeptide coatings can serve as an efficient way to block viral transmission.

The cytotoxicity of the peptides was measured toward both colorectal adenocarcinoma (HT-29) and ovarian carcinoma (A2780) cancer cell lines. The cytotoxicity was tested by using the MTT (3-(4,5-dimethylthiazolyl)-2,5-diphenyltetrazolium bromide) assay after incubation of the cells with the peptides for 24 h. Both peptides showed very low cytotoxicity toward HT-29 cells (Figure 5a). The viability of the more sensitive cells, A2780, was slightly lower for both peptides and reached a plateau at around 60% at high concentrations (Figure 5b). These results suggest that both peptides have low cytotoxicity toward the cells.

3. Conclusion

We show that extremely short peptides, DOPA-Phe-NH2, and DOPA-Phe(4F)-NH2 can spontaneously self-assemble into



ADVANCED MATERIALS INTERFACES

www.advmatinterfaces.de

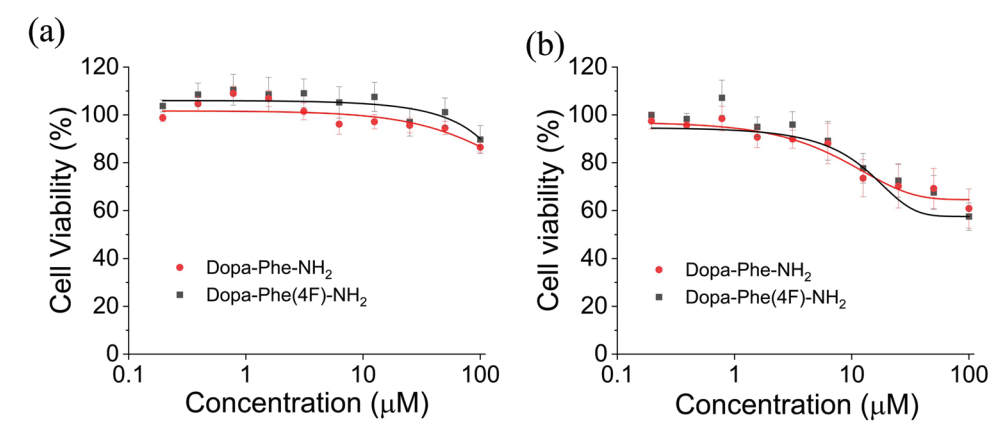


Figure 5. Viability of a) HT-29 and b) A2780 cells based on the MTT assay. Error bars indicate the standard deviations of three independent experiments, n = 3, with triplicates N = 3.

spherical nanoparticles (*tens of nanometers in diameter). These particles exhibit excellent antiviral activity against bacteriophage T4. Although the fluorinated peptide shows better antiviral activity when compared with DOPA-Phe-NH2, our results demonstrate that fluorine is not a necessity for antiviral activity. This is of high importance for some applications. According to the TEM results, the mechanism underlying the antiviral activity could act by disturbing the attached protein between the tail and the head, destroying the long tail fibers that recognize the host cells.^[41,42] We applied the peptide assemblies on a surface by drop-casting to generate a peptide-based coatings. The coating formed by either DOPA-Phe-NH2 or DOPA-Phe(4F)-NH2 exhibited excellent antiviral activity and reduced the number of phages by ≈4 logs. Moreover, the cell viability assay showed that both peptides have very low toxicity against both ovarian carcinoma and colorectal adenocarcinoma cells. Overall, our findings indicate for the first time the use of dipeptide-based assemblies as antiviral agents. This work provides new insights for developing antiviral agents by peptide self-assembly.

4. Experimental Section

Materials: Phe(4F)-Phe(4F)-OMe, DOPA-Phe-NH2, and DOPA-Phe(4F)-NH₂ were purchased from GL Biochem (Shanghai) Ltd. with a purity >95%. L-DOPA with a purity >98% was purchased from Tokyo Chemical Industry Co., Ltd. L-Phenylalanine, L-Phe(4F), and Diphenylalanine (H-Phe-Phe-OH) were purchased from Bachem AG (Bubendorf, Switzerland) Co., Ltd. with a purity of 98%. Methanol, sodium dodecyl sulfate (SDS), ethanol, Roswell Park Memorial Institute (RPMI) 1640 medium, 3-(4,5-dimethylthiazolyl)-2,5-diphenyltetrazolium bromide (MTT) and Isopropanol were obtained from Sigma Aldrich. were purchased from Sigma Aldrich (St. Louis, Missouri, USA). Escherichia coli strain B (Migula) Castellani and Chalmers (ATCC 11303) and E. coli bacteriophage T4 (ATCC 113030-B4) bacteria were purchased from the American Type Culture Collection (ATCC, Manassas, Virginia, USA). Agar and LB broth were purchased from Merck (New Jersey, USA) and Becton Dickinson (New Jersey, USA), respectively. Ovarian carcinoma A2780 was purchased from the European Collection of Authenticated Cell Cultures and colorectal adenocarcinoma HT-29 was purchased from American Type Culture Collection. Fetal Bovine Serum, 1% Penicillin-Streptomycin, and 1% L-Glutamine were purchased from Biological Industries (Beit Haemek, Israel).

Preparation of the Peptide Assemblies and Peptide Coating: The dipeptide assemblies were prepared by dissolving the peptide powder in ethanol at 100 mg mL $^{-1}$; then they were diluted using triple distilled water (TDW) according to our previous work.^[31] The peptide coatings were prepared by drop-casting, on the substrate, 3 times a drop of 100 μ L from a solution of 10 mg mL $^{-1}$ peptide assemblies.

(MIC) Antiviral Minimal Inhibition Concentration Bacteriophage T4: A series of two-fold diluted peptide solutions (1000, 500, 250, 125, 62.5, 31.25, 15.625, and 7.8125 $\mu g \ m L^{-1}$) was prepared to measure the antiviral MIC. Next, 100 µL T4 bacteriophage (10⁵ PFU mL⁻¹) and 100 μL diluted peptide solutions were transferred into 800 µL LB phage; then, the samples were shaken at 150 rpm at room temperature. After 24 h incubation, the samples were centrifuged at 14000×g for 10 min to precipitate the peptide particles. Supernatants were collected and then tenfold diluted once. Next, the 20 µL supernatants were mixed with 25 µL bacteria (E. coli. ATCC11303) in 1 mL of warm 0.6% agarose. The mixture was spread on a 1.5% LB agar to form an agar layer. The plate was incubated at 37 °C for 18 h. The lowest concentration of peptides that prevented viral growth is defined as the antiviral minimum inhibitory concentration (MIC). L-DOPA, L-phenylalanine, L-Phe(4F), Phe(4F)-Phe(4F), and diphenylalanine were used as controls.

Transmission Electron Microscopy (TEM) for the Peptide Assemblies: The peptide assemblies at the antiviral MIC (125 and 62.5 μg mL $^{-1}$ for DOPA-Phe-NH $_2$ and DOPA-Phe(4F)-NH $_2$, respectively) were characterized using Tecnai 12 TEM 120 kV (Phillips, Eindhoven, the Netherlands). A carbon Formvar-coated copper grid was placed on a drop of peptide solution. Then, the samples were negatively stained by adding 5 μL of 2% uranyl acetate for 40 s and dried at room temperature.

Scanning Electron Microscopy (SEM) for the Peptide Assemblies and Coating: SEM analyses were performed by an extra high-resolution scanning electron microscope, Magellan TM400L, operating at 1 kV. A solution of the peptide assemblies at the antiviral MIC (125 and 62.5 $\mu g\ mL^{-1}$ for DOPA-Phe-NH $_2$ and DOPA-Phe(4F)-NH $_2$, respectively) was drop cast on a glass surface and allowed to dry at room temperature. Then, the peptide assemblies and coatings were coated with gold using a Polaron SC7640 sputter coater and then observed.

Atomic Force Microscope (AFM) for the Peptide Assemblies and Coating: The peptide assemblies were prepared at antiviral MIC (125 and 62.5 μg mL⁻¹ for DOPA-Phe-NH₂ and DOPA-Phe(4F)-NH₂, respectively) and then were drop-casted on the clean glass substrate. All AFM images of the peptide assemblies and coatings were taken using AC mode with a Si₃N₂ tip with a spring constant of 3 N m⁻¹ by JPK NanoWizard.

Dynamic Light Scattering (DLS): A Malvern dynamic light scattering (DLS) instrument (Zetasizer Nano ZSZEN3600) was used to determine the size distribution of the peptide assemblies. The size distribution of peptide assemblies at antiviral MIC (125 and 62.5 μg mL⁻¹ for DOPA-Phe-NH₂ and DOPA-Phe(4F)-NH₂, respectively) was performed.





Circular Dichroism (CD): The CD spectra were collected by a J-810 spectropolarimeter (JASCO, Tokyo, Japan), using a 0.1 cm pathlength quartz cuvette for far-UV CD spectroscopy (in the spectral range between 190 and 260 nm with a step width of 0.05 nm) at 20 °C. The peptides were dissolved in TDW (0.1 mg mL $^{-1}$) and then filtered by using a 0.22 μm filter. The spectra for each sample was collected three times, averaged, and the background (TDW) was subtracted.

Fourier Transform Infrared Spectroscopy (FT-IR): FT-IR was recorded using a Nicolet 6700 FT-IR spectrometer with a deuterated triglycine sulfate (DTGS) detector (Thermo Fisher Scientific, MA, USA) at a 4 cm $^{-1}$ resolution and averaged after 2000 scans. Peptide solutions were deposited on a CaF $_2$ plate and dried by vacuum. The peptide deposits were resuspended with D $_2$ O and subsequently dried, forming thin films. The resuspension procedure was repeated twice to ensure maximal hydrogen-to-deuterium exchange.

Attenuated Total Reflection Fourier-Transform Infrared (ATR-FTIR): ATR-FTIR spectra were collected with an applied force of 350 N, at 4 cm $^{-1}$ resolution with 3000 scans averaged signal and an incident angle of 65°.

Transmission Electron Microscopes (TEM) for T4 Bacteriophages: The phage stock solution at a concentration of 1×10^9 PFU mL⁻¹ was diluted to 6×10^7 PFU mL⁻¹ in DDW and added to either the peptide solution or TDW. The final concentration of the peptides DOPA-Phe-NH₂ and DOPA-Phe(4F)-NH₂ was 25 and 12.5 mg mL⁻¹, respectively. The solutions were incubated for 24 h at 37 °C,120 rpm. Then, a 10 μ L drop of each sample was added to the grid for 30 s and the excess was blotted with filter paper. The samples were negatively stained by adding 5 μ L of 2% uranyl acetate for 40 s and the excess was blotted with filter paper.

The samples were analyzed by using Tecnai 12 TEM 120 kV (Phillips, Eindhoven, the Netherlands) equipped with a Phurona camera and RADIUS software (Emsis GmbH, Münster, Germany).

Antiviral Activity against Bacteriophage T4 for Peptide Coatings: The antiviral activity performance was measured according to our previous work.[31] Briefly, 10 decimal serial dilutions of the viral suspension were prepared by LB Broth. The aqueous suspensions for the T4 bacteriophage inactivation experiments contained sample surfaces with dimensions of 1×1 cm and T4 phage at 1.0×10^6 PFU mL⁻¹. Next, the phages were incubated under humid conditions at room temperature (25 °C) in a dark room for 24 h. After incubation, the phages were harvested by shaking them with 2 mL SCDLP broth for 15 min to stop the incubation. The T4 bacteriophage in the SCDLP was diluted with LB broth tenfold. Subsequently, samples and bacteria were mixed with 0.6% agarose. Then, the mixture was spread on 1.5% LB agar to form an agar layer. The plate was incubated at 37 $^{\circ}\text{C}$ for 18 h to form the plaques. The antiviral activity was defined and calculated as follows: The initial virus titer (N_0) and the virus titer after incubation (N) were calculated by counting the plaque number. For each sample, 9 repeats were performed to assess the antiviral activity.

Antiviral activity =
$$log_{10}(N/N_0)$$
 (1)

Antiviral Activity against CCV: The antiviral activity against CCV was performed according to our previous work. [31] Briefly, a drop of 16 μL viral suspension was inoculated onto the coated and uncoated glass surface and incubated for 3 h at room temperature. As a positive control, 16 μL of the viral suspension were added to the glass and incubated for 3 h under UV irradiation (long-wave ultraviolet 365 nm). After the contact time, 2 mL of SCDLP was added to remove the viruses from the surface. From this mixture, a tenfold dilution series was prepared and a TCID $_{50}$ per mL value was determined. Each experiment contained three coated surfaces and three uncoated surfaces, and three experiments were performed.

Cell Culture and Cell Viability Measurements: Colorectal adenocarcinoma (HT-29) and Ovarian carcinoma (A2780) cancer cell lines were cultured as monolayers at 37 °C in a 5% CO $_2$ atmosphere, in RPMI 1640 medium, supplemented with 10% Fetal Bovine Serum, 1% Penicillin-Streptomycin, and 1% L-Glutamine. Cytotoxicity was measured by the previously reported MTT method. [45] The cells were seeded in a 96-well plate, at a density of \approx 10000 cells per well, and allowed to attach overnight under the conditions mentioned above. The

peptides DOPA-Phe-NH2 and DOPA-Phe(4F)-NH2 were dissolved in ethanol to 291 and 276 mm, respectively, and then diluted in TDW to a concentration of 2 mm. The samples were then serially diluted to create a concentration gradient, with pure TDW as the control, and added to the cells so that the highest concentration was set to 100 µm. The plate was incubated for 24 h under the same conditions. MTT, 0.1 mg in 20 µL, was added to each well, followed by an additional 3-h incubation. The medium was removed and 200 µL of isopropanol were added to each well, and the absorbance at 550 nm was measured (Spark 10 M multimode microplate reader spectrophotometer, Tecan Group Ltd., Mannedorf, Switzerland). Cell viability was calculated by comparing the formazan absorbance in the treated wells to the untreated control wells. Each measurement was repeated in three wells per plate, and at least on three different days, to total at least 9 repetitions. The relative IC50 values and the standard error of the means were determined by nonlinear regression of a variable slope (four parameters) model, using the GraphPad Prism 5.0 software.

Statistical Analysis: All measurements were carried out in triplicates on three different days (total of 9 repeats). Values given in the tables and figures are the means of these nine repeats, and error bars indicate the standard deviation. The statistical significance of differences among means was evaluated by Duncan's test at p < 0.05. Statistical analysis was performed using SPSS software version 22.0.

Supporting Information

Supporting Information is available from the Wiley Online Library or from the author.

Acknowledgements

T.H. and M.K. contributed equally to this work. This research was supported by the Ministry of Science & Technology, Israel. T.H. acknowledges the support of the China Scholarship Council (202006760064). The authors would like to thank Dr. Yael Friedmann for her assistance with TEM preparation of the samples and measurements and Ilya Torchinsky for assistance with SEM analysis.

Conflict of Interest

The authors declare no conflict of interest.

Data Availability Statement

The data that support the findings of this study are available from the corresponding author upon reasonable request.

Keywords

antiviral, bacteriophage T4, nanoparticles, peptides, self-assembly

Received: October 1, 2022 Revised: November 21, 2022 Published online: January 29, 2023

^[1] N. Y. Steinman, T. Hu, A. Dombrovsky, M. Reches, A. J. Domb, Biomacromolecules 2021, 22, 4357.

^[2] C. S. Adamson, K. Chibale, R. J. M. Goss, M. Jaspars, D. J. Newman, R. A. Dorrington, *Chem. Soc. Rev.* **2021**, *50*, 3647.





- [3] B. Chen, E.-K. Tian, B. He, L. Tian, R. Han, S. Wang, Q. Xiang, S. Zhang, T. El Arnaout, W. Cheng, Signal Transduct. Target Ther. 2020, 5, 89.
- [4] F. Wu, S. Zhao, B. Yu, Y.-M. Chen, W. Wang, Z.-G. Song, Y. Hu, Z.-W. Tao, J.-H. Tian, Y.-Y. Pei, M.-L. Yuan, Y.-L. Zhang, F.-H. Dai, Y. Liu, Q.-M. Wang, J.-J. Zheng, L. Xu, E. C. Holmes, Y.-Z. Zhang, Nature 2020, 579, 265.
- [5] K. Venkatakrishnan, O. Yalkinoglu, J. Q. Dong, L. J. Benincosa, Clin. Pharmacol. Ther. 2020, 108, 699.
- [6] G. Monteleone, P. C. Sarzi-Puttini, S. Ardizzone, Lancet Rheumatol. 2020, 2, e255.
- [7] F.-D. Cojocaru, D. Botezat, I. Gardikiotis, C.-M. Uritu, G. Dodi, L. Trandafir, C. Rezus, E. Rezus, B.-I. Tamba, C.-T. Mihai, *Pharma-ceutics* 2020, 12, 171
- [8] H. Heydari, R. Golmohammadi, R. Mirnejad, H. Tebyanian, M. Fasihi-Ramandi, M. M. Moghaddam, Peptides 2021, 139, 170526.
- [9] N. Lurie, M. Saville, R. Hatchett, J. Halton, N. Engl. J. Med. 2020, 382, 1969.
- [10] Z. Andreadakis, A. Kumar, R. G. Román, S. Tollefsen, M. Saville, S. Mayhew, Nat. Rev. Drug Discovery 2020, 19, 305.
- [11] S. M. Imani, L. Ladouceur, T. Marshall, R. Maclachlan, L. Soleymani, T. F. Didar, ACS Nano 2020, 14, 12341.
- [12] S. Gurunathan, M. Qasim, Y. Choi, J. T. Do, C. Park, K. Hong, J. H. Kim, H. Song, *Nanomaterials* 2020, 10, 1645.
- [13] H. Huang, C. Fan, M. Li, H.-L. Nie, F.-B. Wang, H. Wang, R. Wang, J. Xia, X. Zheng, X. Zuo, J. Huang, ACS Nano 2020, 14, 3747.
- [14] L. Morawska, J. Cao, Environ. Int. 2020, 139, 105730.
- [15] Z. Sun, K. (K.) Ostrikov, Sustainable Mater. Technol. 2020, 25, e00203
- [16] G. Kampf, D. Todt, S. Pfaender, E. Steinmann, J. Hosp. Infect. 2020, 104, 246.
- [17] E. C. Pirtle, G. W. Beran, Rev. Sci. Tech. 1991, 10, 733.
- [18] O. V. Pyankov, E. V. Usachev, O. Pyankova, I. E. Agranovski, Aerosol Sci. Technol. 2012, 46, 1295.
- [19] J. Haldar, D. An, L. A. de Cienfuegos, J. Chen, A. M. Klibanov, Proc. Natl. Acad. Sci. U. S. A. 2006, 103, 17667.
- [20] F. Yoshie, S. Tetsuya, H. Taishi, N. Tomokazu, N. Mikio, N. Tsuruo, S. Ryuichi, S. Kazuo, Appl. Environ. Microbiol. 2012, 78, 951.
- [21] D. Park, A. M. Larson, A. M. Klibanov, Y. Wang, Appl. Biochem. Biotechnol. 2013, 169, 1134.
- [22] V. Jayawarna, M. Ali, T. A. Jowitt, A. F. Miller, A. Saiani, J. E. Gough, R. V. Ulijn, Adv. Mater. 2006, 18, 611.

- [23] A. Levin, T. A. Hakala, L. Schnaider, G. J. L. Bernardes, E. Gazit, T. P. J. Knowles, *Nat. Rev. Chem.* **2020**, *4*, 615.
- [24] X. Zhao, F. Pan, H. Xu, M. Yaseen, H. Shan, C. A. E. Hauser, S. Zhang, J. R. Lu, *Chem. Soc. Rev.* **2010**, *39*, 3480.
- [25] A. Dehsorkhi, V. Castelletto, I. W. Hamley, J. Pept. Sci. 2014, 20, 453.
- [26] A. Salomé Veiga, J. P. Schneider, Pept. Sci. 2013, 100, 637.
- [27] M. Hughes, S. Debnath, C. W. Knapp, R. V. Ulijn, Biomater. Sci. 2013, 1, 1138.
- [28] K. A. Daher, M. E. Selsted, R. I. Lehrer, J. Virol. 1986, 60, 1068.
- [29] S. Xia, M. Liu, C. Wang, W. Xu, Q. Lan, S. Feng, F. Qi, L. Bao, L. Du, S. Liu, C. Qin, F. Sun, Z. Shi, Y. Zhu, S. Jiang, L. Lu, *Cell Res.* 2020, 30, 343.
- [30] I. Bereczki, M. Csávás, Z. Szűcs, E. Rőth, G. Batta, E. Ostorházi, L. Naesens, A. Borbás, P. Herczegh, ChemMedChem 2020, 15, 1661.
- [31] T. Hu, O. Agazani, S. Nir, M. Cohen, S. Pan, M. Reches, ACS Appl. Mater. Interfaces 2021, 13, 48469.
- [32] J. L. Kyzer, M. Martens, Chem. Res. Toxicol. 2021, 34, 678.
- [33] G. Fichman, L. Adler-Abramovich, S. Manohar, I. Mironi-Harpaz, T. Guterman, D. Seliktar, P. B. Messersmith, E. Gazit, ACS Nano 2014, 8, 7220
- [34] Y. Wang, T. D. Canady, Z. Zhou, Y. Tang, D. N. Price, D. G. Bear, E. Y. Chi, K. S. Schanze, D. G. Whitten, ACS Appl. Mater. Interfaces 2011, 3, 2209
- [35] M. H. Chatain-Ly, S. Moussaoui, V. Rigobello, Y. Demarigny, A. Vera, Front. Microbiol. 2013. 4, 46.
- [36] C. Isanbor, D. O'Hagan, J. Fluorine Chem. 2006, 127, 303.
- [37] M. J. M. Darkes, T. A. Harroun, S. M. A. Davies, J. P. Bradshaw, Biochim. Biophys. Acta, Biomembr. 2002, 1561, 119.
- [38] M. Migliore, A. Bonvicini, V. Tognetti, L. Guilhaudis, M. Baaden, H. Oulyadi, L. Joubert, I. Ségalas-Milazzo, Phys. Chem. Chem. Phys. 2020, 22, 1611.
- [39] P. I. Haris, D. Chapman, Biopolymers 1995, 37, 251.
- [40] D. H. Coombs, F. A. Eiserling, J. Mol. Biol. 1977, 116, 375.
- [41] M. L. Yap, M. G. Rossmann, Future Microbiol. 2014, 9, 1319.
- [42] K. Drexler, J. Dannull, I. Hindennach, B. Mutschler, U. Henning, J. Mol. Biol. 1991, 219, 655.
- [43] M. C. Manning, M. Illangasekare, R. W. Woody, *Biophys. Chem.* 1988, 31, 77.
- [44] S. Maity, S. Nir, T. Zada, M. Reches, Chem. Commun. 2014, 50, 11154
- [45] N. Ganot, S. Meker, L. Reytman, A. Tzubery, E. Y. Tshuva, J. Visualized Exp. 2013, 10, e5076.